
遅延整流性K⁺チャネルの心臓自動能に 果たす役割の検討

(課題番号：11670040)

平成11年度～平成12年度科学研究費補助金(基盤研究(C)(2))研究成果報告書

平成 13 年 3 月

研究代表者 松 浦 博

(滋賀医科大学医学部教授)



2000018548

はしがき

心臓拍動の自動性をもたらす洞房結節細胞の自発性活動電位の発生は、遅延整流性 K^+ チャンネル(I_K)、過分極誘発性内向き陽イオンチャンネル(I_f)、T型ならびにL型 Ca^{2+} チャンネル($I_{Ca,T}$, $I_{Ca,L}$)、dihydropyridide 感受性内向き電流(I_{Na})等の複数のイオンチャンネルの活性の消長によってもたらされていることが明らかにされている。そのうち、 I_K に関して、その活性化は自発性活動電位の最大拡張期電位(約-60 mV)付近までの再分極過程に、またその脱活性化は拡張期緩徐脱分極(ペースメーカー電位)の形成に寄与していることが示されている。

近年、ヒトを含む数種類のは乳類心筋において I_K は電気生理学特性の異なる2種類の電流成分から構成されていることが明らかにされている。すなわち、速い活性化動態をもち強い内向き整流性を示す急速活性型(I_{Kr})とその活性化が比較的遅く内向き整流性の弱い緩徐活性型(I_{Ks})である。また、心臓のイオンチャンネル病として注目を集めている遺伝性QT延長症候群(LQTS)の遺伝子連鎖解析により、 I_{Kr} チャンネルは *KCNH2* (*HERG*)と *KCNE2* の会合により、 I_{Ks} チャンネルは *KCNQ1* (*KvLQT1*)と *KCNE1* の会合によりもたらされ、これらの遺伝子変異に起因してイオンチャンネルの機能障害が出現することが示されている。また、 I_{Kr} と I_{Ks} は異なった薬理学的特性をもち、心臓交感神経伝達物質であるカテコールアミンによる β -アドレナリン性受容体(β -受容体)刺激は I_{Ks} を選択的に増大させること、Vaughan Williams 分類クラスIII群抗不整脈剤であるE-4031, d-sotalol, dofetilide等は、 I_{Kr} を選択的に抑制すること、等が報告されている。これは、神経伝達物質や薬剤による心臓機能(自動能、収縮能)の制御において、 I_{Kr} と I_{Ks} が独自の役割を果たしていることを示すものである。

現在まで、洞房結節の I_{Kr} の特性や自動能に果たす役割について、家兎洞房結節細胞(同細胞では I_K はほぼ I_{Kr} で構成され I_{Ks} がほとんど存在しない)を用いた研究で詳細に検討されてきており、 I_{Kr} は自発性活動電位の再分極過程やペースメーカー電位の形成に中心的な役割を果たしている電流系の一つであることが明らかにされている。我々はモルモット心から単離した洞房結節細胞には I_{Kr} と I_{Ks} の2つの成分がともに存在することを見いだしたので、本研究課題において、モルモット洞房結節細胞を用いて、 I_{Kr} と I_{Ks} の電気生理学的特性や自発性活動電位の発生における役割、さらには受容体、細胞内情報伝達物質による調節機構について検討を行うことにした。モルモット洞房結節細胞における I_{Kr} の電流密度は I_{Ks} の電流密度の約1/20であったが、 I_{Kr} をブロックすると再分極過程後半(-30 mVから最大拡張期電位)の遅延、最大拡張電位の脱分極、さらには自動性の停止が引き起こされ、 I_{Kr} はモルモットにおいても心臓自動性の発生に中心的な役割を果たしていることが判明した。 I_{Ks} をブロックしても最大拡張期電位の脱分極が観察されたため、 I_{Ks} もまた自発性活動電位の再分極過程に寄与していることが示唆された。また、本研究課題では、細胞外ATPによるP2Y代謝調節型受容体-百日咳毒素非感受性G蛋白を介する I_{Ks} の増大機構や細胞内サイクリックGMP(cGMP)による I_{Ks} の調節機構についても検討を加えた。

I_{Kr} と I_{Ks} は種々の伝達物質や薬剤により独自に調節(活性化、抑制)を受けるため、 I_{Kr} と I_{Ks} がともに存在するモルモット洞房結節細胞は、これらの電流の自発性活動電位の発生における独自の役割に関する検討や、神経伝達物質や薬剤による心臓自動能の修飾のメカニズムに関する解析に適した実験モデルと考えられる。

研究組織

研究代表者：松浦 博（滋賀医科大学医学部教授）

研究分担者：尾松万里子（滋賀医科大学医学部助教授）

研究分担者：林 維光（滋賀医科大学医学部助手）

研究経費

平成 11 年度	2,000 千円
平成 12 年度	1,400 千円
計	3,400 千円

研究発表

(1) 学会誌等

Omatsu-Kanbe, M. and Matsuura, H.

Inhibition of store-operated Ca^{2+} entry by extracellular ATP in rat brown adipocytes.

J Physiol 521: 1999, 601-615.（平成 11 年 12 月）

松浦 博, 松林太朗, 額原嗣尚.

心筋活動電位再分極と遅延整流性カリウムチャネルの調節機構.

臨牀と研究 77(4):134-137, 2000.（平成 12 年 4 月）

松浦 博.

情報伝達物質としての ATP 自律神経系：心筋イオンチャネル制御.

生体の科学 2001.（平成 13 年発表予定）

(2) 口頭発表

尾松万里子, 松浦 博

ATP 受容体による容量性 Ca^{2+} 流入機構の抑制

平成 11 年度生理学研究所研究会「ATP 受容体による生理機能制御とその分子的メカニズム」（平成 11 年 8 月 26 日～27 日）

Ding, W.-G., Shimizu, K. and Matsuura, H.

Properties of the delayed rectifier K^{+} current in guinea-pig sino-atrial node pacemaker cells.

第 77 回日本生理学会大会ポスター発表（平成 12 年 3 月 27 日～29 日）

Omatsu-Kanbe, M. and Matsuura, H.

Activation and inhibition of store-operated Ca^{2+} entry (SOCE) in brown adipocytes by ATP.

第 77 回日本生理学会大会ポスター発表（平成 12 年 3 月 27 日～29 日）

Sanada, M., Yasuda, H., Omatsu-Kanbe, M., Matsuura, H. and Kikkawa, R.

Effects of noradrenaline and ATP on cytosolic Ca^{2+} concentration in rat dorsal root ganglion neurons.

第 77 回日本生理学会大会ポスター発表（平成 12 年 3 月 27 日～29 日）

真田 充, 安田 斎, 吉川隆一, 尾松万里子, 松浦 博

ラット脊髄後根神経節細胞に対するノルアドレナリン/ATP の効果：細胞内カルシウム濃度からの検討

第 41 回日本神経学会総会（平成 12 年 5 月 24 日～26 日）

尾松万里子, 松浦 博

PPADS 感受性 ATP 受容体による容量性 Ca^{2+} 流入機構の抑制

平成 12 年度生理学研究所研究会「ATP 受容体による生体機能制御とその分子的メカニズム」（平成 12 年 8 月 24 日～25 日）

Sanada, M., Yasuda, H., Omatsu-Kanbe, M., Matsuura, H. and Kikkawa, R.

Increased depolarization-induced cytosolic Ca^{2+} signal in rat dorsal root ganglion neurons under high glucose with suppressed Na^+/K^+ pump activity.

Fifth Diabetic Neuropathy Satellite（平成 12 年 10 月 31 日～11 月 4 日）

研究成果

本研究課題の成果を要約すると以下の通りである。なお、その詳細は添付した論文に記載する。

モルモット心臓から酵素（コラゲナーゼとエラスラーゼ）処理により得られた単離洞房結節細胞に全細胞型パッチクランプ法(whole-cell recording)を適用して、遅延整流性 K^+ チャネル電流(I_K)の記録(voltage-clamp mode)ならびに自発性活動電位の記録(current-clamp mode)を行った。

1. I_{K1} ならびに I_{Ks} の電気生理学的、薬理学的特性に関する実験 (voltage-clamp mode)

(1) I_K は Vaughan Williams 分類クラス III 群抗不整脈剤である E-4031 (選択的 I_{K1} ブロッカー) 感受性成分(I_{K1})と非感受性成分(I_{Ks})の 2 つの成分から構成されている。

(2) I_{K1} および I_{Ks} の活性化の膜電位依存性は Boltzmann の式でよく fit でき、半最大活性化電位はそれぞれ -26.2 mV および $+17.2 \text{ mV}$ であり、 I_{K1} の方がより過分極電位で活性化された。

(3) I_{K1} ならびに I_{Ks} をほぼ最大に活性化する脱分極パルス (I_{K1} , $+20 \text{ mV}$ へ 500 ms パルス; I_{Ks} , $+70 \text{ mV}$ へ 4000 ms パルス)を与え、続いて保持電位(-50 mV)に再分極したときに発生する末尾電流(tail current)の大きさを細胞膜容量で割って、 I_{K1} ならびに I_{Ks} の電流密度を求めた。 I_{K1} の電流密度 ($0.45 \pm 0.06 \text{ pApF}^{-1}$; $n = 6 \text{ cells}$) は I_{Ks} の電流密度 ($8.71 \pm 0.40 \text{ pApF}^{-1}$; $n = 6 \text{ cells}$) の約 1/20 であったが、活動電位を想定した脱分極パルス ($+20 \text{ mV}$ へ 100 ms パルス)によって活性化される I_{K1} ならびに I_{Ks} の大きさはほぼ等しかった (I_{K1} , $0.38 \pm 0.03 \text{ pApF}^{-1}$; I_{Ks} , $0.43 \pm 0.04 \text{ pApF}^{-1}$; $n = 4 \text{ cells}$)

(4) I_{K1} は強い内向き整流性を示し、一方、 I_{Ks} の電流－電圧関係はほぼ直線状であった。

(5) I_{Ks} は chromanol 誘導体である 293B により可逆的かつ濃度依存性（半最大抑制濃度 = 5.4 μM ）に抑制され、50 μM 以上の濃度でほぼ完全に抑制された。293B による I_{Ks} の抑制効果は脱分極による I_{Ks} の活性化時間の延長とともに強くなった（時間依存性ブロック）

2. 受容体ならびに細胞内情報伝達物質による調節機構について (voltage-clamp mode)

(1) 細胞外 ATP による I_{Ks} の増大反応について

モルモット心房筋細胞および心室筋細胞の場合と同様に、細胞外 ATP は P2Y 代謝調節型受容体—百日咳毒素非感受性 G 蛋白を介して I_{Ks} を増大した。

(2) サイクリック GMP (cGMP) による I_{Ks} の増大反応について

cGMP (100 μM) の細胞内投与ならびに膜透過型 cGMP である 8-bromo-cGMP (100 μM) の細胞外投与はいずれも I_{Ks} に増大効果をおよぼした。その機序を検討した結果、i) phosphodiesterase (type III) の抑制を介するサイクリック AMP (cAMP)—蛋白キナーゼ A 系の活性化と ii) cGMP 依存性蛋白キナーゼ（蛋白キナーゼ G）の活性化の両方を介するものであった。

3. I_{Kr} ならびに I_{Ks} の自発性活動電位の発生における役割について (current-clamp mode)

I_{Kr} ならびに I_{Ks} の自発性活動電位の発生における役割を検討する目的で、current-clamp mode において自発性活動電位を記録しながら、 I_{Kr} もしくは I_{Ks} のブロッカーを作用させその効果を解析した。

(1) I_{Kr} のブロッカーとして E-4031 (0.5 μM) を投与すると、自発性活動電位の再分極過程が約 -30 mV より過分極側で遅延し、続いて最大拡張期電位の脱分極、さらには自発性活動電位の停止が観察された。よって、自発性活動電位の再分極過程後半 (-30 mV 付近から最大拡張電位まで) は主に、 I_{Kr} に依存していることが明らかとなった。

(2) I_{Ks} のブロッカーとして 293B (50 μM) を作用させると、多くの場合、約 10 mV 程度の最大拡張期電位の脱分極が誘発されたので、 I_{Ks} もまた自発性活動電位の再分極過程に寄与していることが示唆された。ただし、293B は開口した I_{Ks} を比較的ゆっくりブロックするので、293B 投与による自発性活動電位発生中の I_{Ks} の抑制の程度に関して今後定量的評価を行い、 I_{Ks} の自発性活動電位の発生における役割について詳細に解析したい。

Rapidly and slowly activating components of delayed rectifier K⁺ current in guinea-pig sino-atrial node pacemaker cells

Hiroshi Matsuura, Tsuguhisa Ehara*, Wei-Guang Ding, Mariko Omatsu-Kanbe
and Takahiro Isono†

*Department of Physiology, †Central Research Laboratory,
Shiga University of Medical Science, Shiga 520-2192 and*

**Department of Physiology, Saga Medical School, Saga 849-8501, Japan*

Running title: I_{Kr} and I_{Ks} in sino-atrial node cells

Key words; Sino-atrial node; Delayed rectifier; Potassium current

Name and address for correspondence and proofs:

Dr. Hiroshi Matsuura,

Department of Physiology,

Shiga University of Medical Science,

Otsu, Shiga 520-2192, Japan

Tel: 077 548 2151

Fax: 077 543 1960

International Code (+81 77)

E-mail: matuurah@belle.shiga-med.ac.jp

SUMMARY

1. The components and properties of the delayed rectifier K^+ current (I_K) in isolated guinea-pig sino-atrial (SA) node pacemaker cells were investigated using the whole-cell configuration of the patch-clamp technique.
2. An envelope of tails test was conducted by applying depolarizing pulses from a holding potential of -50 mV to +40 mV for various durations ranging from 20 to 2000 ms. The ratio of the tail current amplitude elicited upon return to the holding potential to the magnitude of the time-dependent outward current activated during depolarizing steps changed depending on the pulse duration, while after exposure to 5 μ M E-4031, this current ratio became constant irrespective of the pulse duration. These observations are consistent with the presence of drug-sensitive, rapidly activating and drug-resistant, slowly activating components of I_K (I_{Kr} and I_{Ks} , respectively) in guinea-pig SA node cells.
3. The activation range for I_{Kr} , defined as the E-4031-sensitive current (half-activation voltage, $V_{1/2}$, of -26.2 mV) was much more negative than that for I_{Ks} , defined as the E-4031-resistant current ($V_{1/2}$ of +17.2 mV). I_{Kr} exhibited a marked inward rectification at potentials positive to -50 mV, whereas I_{Ks} showed only a slight rectification.
4. The tail current amplitude of I_{Kr} was similar to that of I_{Ks} , when measured upon repolarization to -50 mV after a 100-ms depolarizing pulse to +20 mV, simulating an action potential.
5. In the current-clamp experiment, a bath application of E-4031 (0.5 and 5 μ M) initially delayed the repolarization at potentials negative to approximately -30 mV and depolarized the maximum diastolic potential, followed by the arrest of spontaneous activity, thus indicating that the late phase of the repolarization leading to the maximum diastolic potential at around -60 mV in spontaneous action potentials is primarily produced by I_{Kr} in guinea-pig SA node cells.
6. These results provide evidence to suggest that I_{Kr} is present and plays a crucial role in the spontaneous activity of guinea-pig SA node pacemaker cells.

INTRODUCTION

The spontaneous activity of the sino-atrial (SA) node pacemaker cells in the mammalian heart has been demonstrated to be generated by the interaction of multiple ionic currents (for a review see Irisawa *et al.* 1993); an inward current is provided by the hyperpolarization-activated current (I_f ; DiFrancesco *et al.* 1986), the background non-selective cation current (Hagiwara *et al.* 1992), the sustained inward current (Guo *et al.* 1995) and the T- and L-type Ca^{2+} currents ($I_{\text{Ca,T}}$ and $I_{\text{Ca,L}}$, respectively; Hagiwara *et al.* 1988; Doerr *et al.* 1989), while the delayed rectifier K^+ current (I_K) mainly contributes the outward current for the generation of pacemaking activity in SA node cells under physiological conditions. Spontaneous openings of the muscarinic K^+ channels are also known to produce a substantial outward current which may affect the electrical activity of the pacemaker cells (Ito *et al.* 1994). The activation of I_K during the plateau phase of spontaneous action potentials plays an important role in the repolarization of the cell membrane toward the K^+ equilibrium potential, while a gradual deactivation of I_K at negative potentials during membrane repolarization, together with the activation of the inward currents, is responsible for generating the slow diastolic depolarization (pacemaker potential). I_K thus plays a crucial role not only in the repolarization phase but also in the pacemaker depolarization in the spontaneous action potentials of SA node cells.

Electrophysiological and pharmacological studies have revealed two kinetically and pharmacologically distinct components of I_K in atrial and ventricular myocytes of a variety of mammalian species, including guinea-pig (Sanguinetti & Jurkiewicz, 1990a, 1990b, 1991), dog (Liu & Antzelevitch, 1995; Gintant, 1996) and humans (Wang *et al.* 1994; Li *et al.* 1996). I_{Kr} activates rapidly in response to depolarization to levels positive to -40 mV, displays a marked inward rectification, and is specifically blocked by lanthanum ions and by methanesulfonanilide class III antiarrhythmic drugs such as E-4031, sotalol and dofetilide. In contrast, I_{Ks} activates more slowly and at more depolarized potentials, shows a weak inward rectification and is resistant to these drugs. In recent years, evidence has been presented regarding the molecular structures of these two

distinct I_K channels; HERG coassembles with the minK-related peptide 1 (MiRP1) to form I_{Kr} channels (Curran *et al.* 1995; Sanguinetti *et al.* 1995; Trudeau *et al.* 1995; Abbott *et al.* 1999), whereas, in coassembly with the minK, K_vLQT1 encodes the I_{Ks} channels (Barhanin *et al.* 1996; Sanguinetti *et al.* 1996).

It has yet to be fully elucidated as to whether these two components of I_K are distributed in the SA node pacemaker cells of mammalian species. Previous studies on I_K in this cell type have been mostly confined to the rabbit heart, and in this preparation it has been shown that I_{Kr} is readily distinguished and is essential for the development of spontaneous action potentials (Shibasaki, 1987; Ono & Ito, 1995; Verheijck *et al.* 1995; Lei & Brown, 1996). However, such a functional role for I_{Kr} in the SA node pacemaking activity has not yet been studied in detail in other mammalian species. In guinea-pig SA node cells, on the other hand, I_K has been reported to be largely composed of one component which resembles I_{Ks} (Anumonwo *et al.* 1992; Freeman & Kass, 1993). The present study was undertaken to characterize the components and properties of I_K in isolated SA node pacemaker cells of guinea-pig using the whole-cell patch-clamp technique together with a potent methanesulfonanilide I_{Kr} blocker E-4031. Our results provide the first detailed evidence to show that I_{Kr} is indeed present and plays a central role in the late repolarization in spontaneously contracting SA node cells of the guinea-pig heart.

METHODS

SA node cell isolation

Single SA node cells were isolated from the hearts of guinea-pigs (250-400 g body weight) using an enzymatic dissociation procedure similar to that described previously (Guo *et al.* 1997). Briefly, guinea-pigs were deeply anaesthetized with an overdose of sodium pentobarbitone (≥ 120 mg kg⁻¹, i.p.) and then the chest cavity was opened under artificial respiration. The ascending aorta was cannulated *in situ* and the heart was then excised and retrogradely perfused via the aortic cannula on a Langendorff apparatus at 37 °C, initially for 4 min with normal Tyrode solution and then for 4 min with nominally Ca²⁺-free Tyrode solution. This was followed by 8-12 min of perfusion with nominally Ca²⁺-free Tyrode solution containing 0.4 mg ml⁻¹ collagenase (Wako Pure Chemical Industries, Osaka, Japan). All these solutions were oxygenated with 100% O₂. The digested heart was then removed from a Langendorff apparatus, and the SA node region was dissected out and cut perpendicular to the crista terminalis into small strips measuring about 0.5 mm in width. These SA node tissue strips were further digested at 37 °C with nominally Ca²⁺-free Tyrode solution containing 1.0 mg ml⁻¹ collagenase and 0.1 mg ml⁻¹ elastase (Boehringer Mannheim, Germany) for 20 min. Finally, the enzyme-digested SA node strips were mechanically agitated in a high-K⁺, low-Cl⁻ Kraftbrühe (KB) solution (Isenberg & Klöckner, 1982) to disperse the cells. The isolated cells thus obtained were then stored at 4 °C in the KB solution until use. All these experimental procedures were reviewed and approved by the Shiga University of Medical Science Animal Care Committee.

Whole-cell patch clamp technique and data analysis

The membrane potentials and whole-cell currents were recorded using the whole-cell patch-clamp technique (Hamill *et al.* 1981) under the current- and voltage-clamp mode, respectively. An EPC-7 patch-clamp amplifier (List-electronic, Darmstadt, Germany) was used for these recordings. The patch electrodes were fabricated from glass capillaries (outside diameter 1.5 mm; Narishige

Scientific Instrument Lab., Tokyo, Japan) using a three-stage horizontal microelectrode puller (P-80; Sutter Instrument Co., Novato, CA, USA), and the tips were then fire-polished with a microforge. Electrode resistance ranged from 2.0 to 4.0 M Ω when filled with the pipette solution. Aliquots of cells were transferred to a recording chamber (0.5 ml in volume) mounted on the stage of an inverted microscope (TMD300, Nikon, Tokyo) and were superfused at a constant flow rate of 2 ml min⁻¹ with normal Tyrode solution at 35-37 °C. After a tight seal (resistance, 5 to 50 G Ω) was established between the electrode tip and the cell membrane by gentle suction (-20 to -30 cm H₂O), the membrane patch was then ruptured by a brief period of more vigorous suction, controlled manually with a 2.5-ml syringe.

The SA node cells were identified based on the presence of both spontaneous action potentials recorded in the current-clamp mode and the hyperpolarization-activated inward current (I_p) recorded in the voltage-clamp mode during superfusion with normal Tyrode solution. I_K was activated by the depolarizing test pulses, under conditions where the Na⁺ channels (I_{Na}) were inactivated by setting the holding potential to -40 or -50 mV and the L-type Ca²⁺ channels (I_{CaL}) were blocked by adding 0.4 μ M nisoldipine to the normal Tyrode solution. Nisoldipine was shown to have no effect on the cardiac I_K at this concentration (Sanguinetti & Jurkiewicz, 1991).

The current and voltage signals were stored on a digital audiotape (DM120, Hitachi maxell, Tokyo, Japan) using a PCM data recorder (RD-101T, TEAC, Tokyo, Japan) and were later fed to the computer (PC98RL, NEC, Tokyo, Japan) every 1 ms through a low-pass filter (48 dB per octave, E-3201A, NF, Yokohama, Japan) at an appropriate cut-off frequency (usually 3 kHz) for data analysis. Cell membrane capacitance (C_m) was calculated from the capacitive transients elicited by 20-ms voltage-clamp steps (± 5 mV) according to the relationship: $C_m = \tau_c I_0 / \Delta V_m (1 - I_\infty/I_0)$, where τ_c is the time constant of the capacitive transient, I_0 is the initial peak current amplitude, ΔV_m is the amplitude of voltage step (± 5 mV) and I_∞ is the steady-state current value. The average capacitance value for SA node cells used in the present study was 38.9 ± 1.8 pF (mean \pm S.E.M.; $n = 15$ cells). The tail current amplitude of I_{Kr} and I_{Ks} was divided by the cell capacitance to provide an estimate of current density (pA pF⁻¹).

The results were expressed as the mean \pm S.E.M.; n indicates the number of cells studied. Statistical comparisons were made using the Student's t test, and differences were regarded as significant at the 95 % confidence level.

Solutions and chemicals

Normal Tyrode solution contained (in mM) 140 NaCl, 5.4 KCl, 1.8 CaCl₂, 0.5 MgCl₂, 0.33 NaH₂PO₄, 5.5 glucose, and 5.0 HEPES (pH adjusted to 7.4 with NaOH). The nominally Ca²⁺-free Tyrode solution used for isolating the cells was prepared by simply omitting CaCl₂ from the normal Tyrode solution. The extracellular solution used for measuring whole-cell I_K was normal Tyrode solution supplemented with 0.4 μ M nisoldipine (a generous gift from Bayer, Germany). Nisoldipine was prepared as a 1-mM stock solution in ethanol. The HCl-salt of E-4031 (N-[4-[[1-[2-(6-methyl-2-pyridinyl)ethyl]-4-piperidinyl]carbonyl]phenyl]methanesulfonamide dihydrochloride dihydrate; a generous gift from Eisai Pharmaceutical Co., Tokyo, Japan) was dissolved in distilled water as a 1-mM stock solution and then was added to the extracellular solution to give a final concentration of either 0.5 or 5 μ M in some experiments as indicated. The pipette solution contained (in mM) 70 K-aspartate, 50 KCl, 10 KH₂PO₄, 1 MgSO₄, 3 Na₂-ATP, 0.1 Li₂-GTP, 5 EGTA, 2 CaCl₂, 5 HEPES (pH adjusted to 7.2 with KOH). The concentration of free Ca²⁺ in the pipette solution was estimated to be approximately 0.1 μ M. The KB solution for cell preservation contained (in mM) 70 K-glutamate, 30 KCl, 10 KH₂PO₄, 1 MgCl₂, 20 taurine, 0.3 EGTA, 10 glucose, and 10 HEPES (pH adjusted to 7.2 with KOH).

RESULTS

Characteristics of guinea-pig SA node pacemaker cells

Figure 1 near here

When single cells enzymatically dissociated from the SA node region of the guinea-pig heart were superfused with normal Tyrode solution, less than 5% of total cells only showed spontaneous and regular contraction. These pacemaker SA node cells were typically spindle-shaped with faint striations and had a small bulge around their center. Such a scarce presence of pacemaker SA node cells in guinea-pig heart appears to be consistent with the previous morphological examination demonstrating that the amount of cells in the primary pacemaker area of the guinea-pig (less than 1000 cells) was much less than that of the rabbit (about 5000 cells; Bleeker *et al.* 1980; Opthof *et al.* 1985). In the present study, all electrophysiological recordings were made from these spontaneously and regularly contracting SA node cells.

Figure 1 demonstrates a representative recording of membrane potential and whole-cell currents of an isolated guinea-pig SA node cell superfused with normal Tyrode solution. As illustrated in Fig. 1A, the SA node cell exhibited spontaneous action potentials that arose smoothly from the preceding slow diastolic depolarization (pacemaker depolarization). The spontaneous contraction rate and maximum diastolic potential recorded from isolated guinea-pig SA node cells were 205 ± 11 min⁻¹ and -59.3 ± 1.8 mV ($n = 20$ cells), respectively, which are comparable to those of rabbit SA node cells (Ono & Ito, 1995; Verheijck *et al.* 1995). Figure 1B shows membrane currents in response to 500-ms depolarizing (up to +40 mV) and hyperpolarizing test pulses (up to -120 mV) applied in 10 mV steps from a holding potential of -40 mV. The depolarizing clamp steps first activated an inward current which peaked at potentials around 0 mV (Fig. 1C) and was sensitive to inhibition by 0.4 μ M nisoldipine (cf. Fig 3A), thus confirming that the inward current is due to the L-type Ca²⁺ current ($I_{Ca,L}$). During depolarization the inactivation of the inward $I_{Ca,L}$ was followed

by the time-dependent increase in outward current representing an activation of I_K , while a slowly decaying outward tail current associated with the deactivation of I_K was observed after a return to a holding potential of -40 mV (Fig. 1B).

Changes in the membrane currents in response to hyperpolarizing pulses were characterized by an instantaneous current jump of small amplitude in the inward direction followed by the time- and voltage-dependent activation of the inward current (Fig. 1B), thus showing that the hyperpolarization-activated inward current (I_p) is present while the inward rectifier K^+ current (I_{K1}) is either absent or, if any, very small in guinea-pig SA node pacemaker cells. The activation of I_p , detected as the difference between the initial (●) and late current levels (○) during hyperpolarizations, became evident at levels negative to -60 mV (Fig. 1C).

Two components of I_K revealed by the envelope of tails test

Figure 2 near here

We next examined the components and properties of I_K in guinea-pig SA node pacemaker cells, under conditions in which $I_{Ca,L}$ was blocked by adding 0.4 μ M nisoldipine to the normal Tyrode solution. An envelope of tails test (Noble & Tsien, 1969) was conducted to clarify whether I_K arises from a single or multiple component of I_K . An SA node pacemaker cell was depolarized from a holding potential of -50 mV to +40 mV for various durations ranging from 20 to 2000 ms (Fig. 2A, top) and the magnitude of the tail current ($I_{K,tail}$) elicited upon repolarization to the holding potential after the depolarizing test pulses was compared with the magnitude of the outward current ($I_{K,pulse}$) activated during depolarization for each test pulse duration ($n = 3$ cells). The $I_{K,tail}$ elicited following brief depolarizations (20 and 60 ms) was consistently greater than $I_{K,pulse}$, while $I_{K,pulse}$ predominated over $I_{K,tail}$ at longer pulse durations (≥ 100 ms). The ratio of $I_{K,tail}$ to $I_{K,pulse}$ progressively declined with the lengthening of the pulse duration and reached a practically steady value of about 0.5 at 500 ms pulse (○, Fig. 2B). The ratio was thus dependent upon the duration

of pulse, suggesting the presence of more than one component of I_K in SA node cells. After I_{Kr} was selectively blocked by exposure to 5 μ M E-4031, the ratio of $I_{K,tail}$ to $I_{K,pulse}$, obtained from the same cell, became constant at approximately 0.35, regardless of the pulse duration (●, Fig. 2B), suggesting that only one component remains in the presence of the drug. These observations are consistent with the presence of the drug-sensitive (I_{Kr}) and drug-resistant components (I_{Ks}) of I_K in guinea-pig SA node pacemaker cells.

Electrophysiological properties of I_{Kr} in guinea-pig SA node cells

Figure 3 near here

We investigated the electrophysiological properties of I_{Kr} , determined as an E-4031 sensitive current, in an SA node cell. Figure 3 shows a representative analysis of the voltage-dependence of I_{Kr} activation. I_K was activated by 500-ms depolarizing steps to membrane potentials between -40 and +20 mV in the absence (Fig. 3A, middle) and the presence of 5 μ M E-4031 (bottom), and I_{Kr} at each test potential was obtained by digitally subtracting I_K in the presence of E-4031 from that in its absence (Fig. 3B). The activation of I_{Kr} in response to depolarizing steps was relatively rapid, reaching a steady level after a few hundred milliseconds (Fig. 3B). The voltage dependence of I_{Kr} activation was evaluated by measuring the amplitude of I_{Kr} tail current elicited on return to -50 mV, which reflects the degree of activation at the preceding depolarizing test potential ($n = 3$ cells). The activation variable (n_∞) was then obtained by normalizing the amplitude of the tail current at each test potential with reference to its peak amplitude obtained at +20 mV, and was plotted as a function of membrane potential to obtain the steady-state activation curve. The relationship between n_∞ and the test potential was reasonably fitted by a Boltzmann equation:

$$n_\infty = 1 / [1 + \exp\{(V_{1/2} - V_m)/k\}] \quad (1)$$

where V_m is the test potential, $V_{1/2}$ is the voltage at which the activation is half-maximal (-26.2 mV), and k is the slope factor (8.7 mV). The values of $V_{1/2}$ and k are comparable to those reported for I_{Kr} in other cardiac preparations including guinea-pig atrial cells ($V_{1/2}$, -19.3 mV; k , 5.2 mV; Sanguinetti & Jurkiewicz, 1991), guinea-pig ventricular cells ($V_{1/2}$, -21.5 mV; k , 7.5 mV; Sanguinetti & Jurkiewicz, 1990a), rabbit SA node cells ($V_{1/2}$, -25.1 mV; k , 7.4 mV; Shibasaki, 1987; $V_{1/2}$, -23.2 mV; k , 10.6 mV; Ono & Ito, 1995), human atrial cells ($V_{1/2}$, -14.0 mV; k , 6.5 mV; Wang *et al.* 1994), and human ventricular cells ($V_{1/2}$, -14.0 mV; k , 7.7 mV; Li *et al.* 1996). The current density of I_{Kr} , obtained by normalizing the peak amplitude of I_{Kr} tail current measured upon return to the -50 mV holding potential following depolarization to $+20$ mV with reference to the cell capacitance, was 0.45 ± 0.03 pA pF $^{-1}$ ($n = 6$ cells).

Figure 4 near here

A relatively small outward current of I_{Kr} activated during depolarizing steps was unchanged or somewhat reduced in amplitude with the increasing magnitude of depolarization to positive potentials (Fig. 3B). This observation is consistent with the presence of the inward rectifying property of I_{Kr} , which has been proposed to result from a rapid inactivation in response to membrane depolarization (Shibasaki, 1987; Sanguinetti & Jurkiewicz, 1990a; Ono & Ito, 1995; Sanguinetti *et al.* 1995; Smith *et al.* 1996; Spector *et al.* 1996). We assessed the conductance properties of I_{Kr} in guinea-pig SA node pacemaker cells by measuring the amplitude of outward tail currents during the double pulse protocol; the cell was first depolarized to $+20$ mV for 500 ms to fully activate I_{Kr} (cf. Fig. 3C), and then was repolarized to potentials ranging from $+10$ to -70 mV before (○) and during (●) the exposure to 5 μ M E-4031 (Fig. 4A). It should be noted that membrane currents during hyperpolarization to -70 mV both in the absence and presence of E-4031 exhibited a time-dependent increase in the inward direction, which appears to reflect the activation of I_f . An outward tail current of I_{Kr} at each test potential was measured as the E-4031-sensitive current, obtained by the digital subtraction of the current trace in the presence of E-4031 from that in its absence. The I_{Kr} tail

current was not detected at +10 mV but did become evident at negative potentials (≤ -10 mV, Fig. 4B). The amplitude of I_{Kr} tail current at around and negative to E_K was too small to be accurately isolated by use of this subtraction method with a concomitant activation of I_f which frequently exhibited a run-down during the course of experiments (DiFrancesco *et al.* 1986; Ono & Ito, 1995). The voltage dependence of the peak amplitude of I_{Kr} tail current is illustrated in Fig. 4C, which clearly shows a prominent inward rectification at potentials positive to -50 mV. Given that this inward rectification is due to the voltage-dependent inactivation of the channel, the amplitude of I_{Kr} can be described as

$$I_{Kr} = G_{Kr} P_{i,\infty} (V_m - E_R) \quad (2)$$

and

$$P_{i,\infty} = 1 / (1 + \exp[(V_m - V_{1/2})/k]) \quad (3)$$

where G_{Kr} is the maximum conductance of I_{Kr} , $P_{i,\infty}$ is the steady-state inactivation given by the Boltzmann equation (3), $V_{1/2}$ is the voltage at which steady-state inactivation is half maximal, k is the slope factor, and E_R is the reversal potential. Assuming E_R to be -85 mV, a calculated equilibrium potential for K^+ under the present experimental conditions (Sanguinetti & Jurkiewicz, 1990a, 1991; Ono & Ito, 1995), the data points could be reasonably fitted by Eqs (2) and (3) with $V_{1/2}$ of -35.4 mV and k of 13.4 mV. These parameters related to voltage dependence of I_{Kr} inactivation are comparable to those reported for I_{Kr} in other cardiac preparations (I_{Kr} in the rabbit SA node, $V_{1/2}$, -28.6 mV, k , 17.1 mV; Ono & Ito, 1995; $V_{1/2}$, -42.1 mV, k , 9.35 mV; Ho *et al.* 1996).

Properties of I_{Ks} in guinea-pig SA node cells

Figure 5 near here

The voltage-dependence of I_{Ks} activation was examined by measuring the amplitude of the outward tail currents elicited upon return to the -50 mV holding potential after 4-s depolarizing test pulses to various potentials in the presence of 5 μ M E-4031 (Fig. 5A). The activation variable (n_∞) for I_{Ks} was calculated by normalizing the amplitude of I_{Ks} tail current at each test potential with respect to its peak amplitude obtained at +70 mV and then was plotted as a function of the test potential (Fig. 5B). A continuous curve through the data points shows the least-squares fit of a Boltzmann equation (Eq 1), yielding $V_{1/2}$ of +17.2 mV and k of 13.5 mV. These values were similar to those reported for I_{Ks} in atrial ($V_{1/2}$, 24.0 mV; k , 15.7 mV; Sanguinetti & Jurkiewicz, 1991) and ventricular myocytes ($V_{1/2}$, 15.7 mV; k , 12.7 mV; Sanguinetti & Jurkiewicz, 1990a) of guinea-pig. The current density of I_{Ks} , obtained by normalizing the amplitude of the peak tail current elicited upon return to the -50 mV holding potential following depolarization to +70 mV with reference to the cell capacitance, was 8.71 ± 0.40 pA pF⁻¹ ($n = 6$ cells).

Figure 6 near here

We next examined the fully-activated I - V relationship of I_{Ks} in guinea-pig SA node pacemaker cells. For this purpose, the cell was first depolarized to +40 mV for 4 s, and was then repolarized to potentials ranging from +30 to -110 mV in the presence of 5 μ M E-4031 to abolish I_{Kr} (Fig. 6A; left column). The decaying outward current elicited at potentials ≥ -50 mV can be regarded as solely representing the deactivation of I_{Ks} , whereas the time-dependent change in the membrane currents observed at potentials ≤ -60 mV appears to arise not only from the deactivation of I_{Ks} but also from the activation of I_f (cf. Fig. 1B & C). The deactivation of I_{Ks} elicited at potentials ≤ -60 mV after depolarization to +40 mV (Fig. 6A; right panel) was therefore isolated by subtracting I_f activated by hyperpolarization from a holding potential of -50 mV (middle panel) from the membrane current elicited upon hyperpolarization from +40 mV (left panel). The amplitude of I_{Ks} tail current was then divided by the expected changes in the activation variable (n_∞) for I_{Ks} (Fig. 5B) and plotted against the membrane potential (Fig. 6B). The fully-activated I - V relationship for I_{Ks} was nearly linear in

the potential range between -110 and -30 mV and rectified slightly in the inward direction at more positive potentials, similar to the conductance property of I_{Ks} previously recorded in other cardiac cell types (Matsuura *et al.* 1987; Sanguinetti & Jurkiewicz, 1991; Zhou & Lipsius, 1994). In addition, I_{Ks} tail current reversed its polarity at -81.2 ± 2.5 mV ($n = 3$ cells), which is close to the predicted equilibrium potential for K^+ (-85 mV), indicating that I_{Ks} was predominantly carried by K^+ ions, as has previously been demonstrated in guinea-pig atrial cells (Sanguinetti & Jurkiewicz, 1991).

Role of I_{Kr} in the spontaneous activity of guinea-pig SA node cells

Figure 7 near here

Voltage-clamp experiments so far described in the present study provide evidence for the presence of I_{Kr} as well as I_{Ks} in guinea-pig SA node pacemaker cells. In order to elucidate whether I_{Kr} contributes to the spontaneous pacemaker activity of SA node cells, we examined the effect of the block of I_{Kr} on spontaneous action potentials. Figure 7 illustrates a representative example of the effects of E-4031 at $0.5 \mu\text{M}$, a concentration known to produce more than 50 % inhibition of I_{Kr} without affecting other ionic currents (Sanguinetti & Jurkiewicz, 1990a; Ito & Ono, 1995; Verheijck *et al.* 1995). Under control conditions, an SA node cell exhibited regular and stable pacemaker activity with a contraction rate of 262 min^{-1} and a maximum diastolic potential of -61 mV (Fig. 7B, upper panel, ○). An application of $0.5 \mu\text{M}$ E-4031 initially delayed the repolarizing phase of the action potentials at levels negative to approximately -30 mV and depolarized the maximum diastolic potential (Fig. 7B, upper panel, ●). These effects of E-4031 were followed by either a cessation of the spontaneous activity which was observed in most of the cells examined (5 out of 7 cells; Fig. 7A), or an irregular and decelerated firing of the action potentials in the remaining cells (2 out of 7 cells). The membrane potential of the cells in which spontaneous activity was abolished during exposure to E-4031 was stabilized at -30.1 ± 2.8 mV (Fig. 7A; $n = 5$ cells). The gradual hyperpolarization of membrane potential observed after washing off the drug appears to reflect the

recovery of I_{Kr} from the block by E-4031. The cell eventually restored its regular and stable spontaneous action potentials with contraction rate of 255 min^{-1} and maximum diastolic potential of -59 mV , about 6 min after washing off the drug (Fig. 7B, lower panel, ■). Higher concentration ($5 \mu\text{M}$) of E-4031 also preferentially affected the late repolarization phase at first and then induced a rapid and complete arrest of the electrical activity in all cells examined ($n = 3$), which was not reversed after washing out the drug (data not shown). These results strongly suggest that I_{Kr} contributes primarily to the late phase of repolarization and that blocking I_{Kr} leads to either an arrest or deceleration of the spontaneous activity in guinea-pig SA node cells.

Figure 8 near here

The tail current amplitude of fully activated I_{Kr} ($0.45 \pm 0.03 \text{ pA pF}^{-1}$; $n = 6$ cells, cf. Fig. 3) was about 5% that of the fully activated I_{Ks} ($8.71 \pm 0.40 \text{ pA pF}^{-1}$; $n = 6$ cells, cf. Fig. 5) in guinea-pig SA node pacemaker cells. However, I_{Kr} activates more rapidly and at more negative potentials than I_{Ks} , favoring the contribution of I_{Kr} to providing the repolarizing outward current during the action potential. We therefore compared the amplitude of I_{Kr} and I_{Ks} during the voltage-clamp protocol simulating the action potential (100-ms depolarization to $+20 \text{ mV}$ followed by repolarization to -50 mV) in the experiments shown in Fig. 8. I_{Kr} was defined as an E-4031-sensitive I_K (Fig. 8B) obtained by digital subtraction of I_K in the presence of $5 \mu\text{M}$ E-4031 from that in its absence (C-E, Fig. 8A), while I_{Ks} was detected as an E-4031-resistant I_K (denoted as E in Fig. 8A). The tail currents of I_{Kr} and I_{Ks} elicited upon repolarization to -50 mV were found to be of a similar magnitude (Fig. 8C; I_{Ks} , $0.38 \pm 0.03 \text{ pA pF}^{-1}$; I_{Kr} , $0.43 \pm 0.04 \text{ pA pF}^{-1}$; $n = 4$ cells).

DISCUSSION

The present investigation characterized I_K in spontaneously active SA node cells in the guinea-pig heart using a methanesulfonanilide class III antiarrhythmic agent E-4031, which has been demonstrated to specifically inhibit I_{Kr} in cardiac myocytes (Sanguinetti & Jurkiewicz, 1990a, 1991). Under control conditions, I_K does not satisfy the envelope of tails test, consistent with the activation of more than one current system exhibiting distinct properties of kinetics and conductance (Noble & Tsien, 1969), whereas after the blockade of I_K sensitive to E-4031, the remaining I_K completely satisfies the test, supporting the view that only a single current system exists during the exposure to E-4031 (Fig. 2). This test clearly indicates that I_K in guinea-pig SA node pacemaker cells is generated by activation of both the drug-sensitive and drug-resistant I_K (I_{Kr} and I_{Ks} , respectively). In addition, the ratio (0.35) of the tail current to time-dependent current for I_{Ks} , recorded in the presence of E-4031 (●, Fig. 2B), is slightly larger than the predicted ratio (0.26) of the driving force at +40 and -50 mV for a non-rectifying membrane current having the reversal potential of -81 mV, which can be accounted for by the presence of a weak inward rectification in I_{Ks} (Fig. 6).

Sanguinetti & Jurkiewicz (1990a, 1990b, 1991) have shown that I_K in guinea-pig atrial and ventricular myocytes can be divided into two distinct components by a sensitivity to inhibition by lanthanum ions and by methanesulfonanilide E-4031; I_{Kr} , defined as the drug-sensitive current, exhibits a rapid activation and a marked inward rectification, whereas I_{Ks} , defined as a drug-resistant current, activates more slowly and exhibits a slight rectification. These two distinct components of I_K have since been identified in atrial and ventricular myocytes of various mammalian species including human (Wang *et al.* 1994; Liu & Antzelevitch, 1995; Gintant, 1996; Li *et al.* 1996).

Previous studies investigating the composition and properties of I_K in mammalian pacemaker cells were mostly undertaken using rabbit SA node cells. In this preparation, the exposure to E-4031 has been demonstrated to nearly completely abolish I_K (Ono & Ito, 1995; Verheijck *et al.* 1995; Ho *et al.* 1995), thus suggesting that I_{Kr} is a predominant component of I_K in rabbit SA node cells. These studies further demonstrated that a bath application of E-4031 prolonged the action potential

duration, depolarized the maximum diastolic potential, and eventually abolished the spontaneous activity, indicating that I_{Kr} is essential for maintaining the SA node automaticity. In recent years, Lei & Brown (1996) showed that a part of I_K is resistant to dofetilide at 1 μ M, a concentration known to completely abolish cardiac I_{Kr} (Carmeliet 1992), and that the dofetilide-resistant I_K shows the electrophysiological properties which are comparable to I_{Ks} previously recorded in other cardiac cells, such as a half-activation voltage of 15.6 mV and a slope factor of 14.7 mV, thus suggesting that I_{Ks} is also present in rabbit SA node cells.

On the other hand, it has been demonstrated in guinea-pig SA node pacemaker cells that I_K activates at potentials positive to -20 mV and is little affected by exposure to either E-4031 (5 μ M) or lanthanum ions (100 μ M). In addition, I_K has been shown to satisfy the envelope of tails test with the ratio of tail current to time-dependent current expected for a slightly rectifying current system (Anumonwo *et al.* 1992; Freeman & Kass, 1993). These observations indicate that I_{Ks} is the major component of I_K in this preparation. In the present study, we consistently detected an E-4031-sensitive current which activates rapidly, reaching a steady-state within 200-300 ms after depolarization (Fig. 3), and displays a marked inward rectification at depolarized potentials (Fig. 4) in spontaneously active SA node cells of the guinea-pig heart. We found that I_{Kr} current density (0.45 ± 0.03 pA pF⁻¹; n = 6 cells) is approximately one-twentieth of I_{Ks} current density (8.71 ± 0.40 pA pF⁻¹; n = 6 cells) in guinea-pig SA node cells, and this small amplitude of I_{Kr} relative to large I_{Ks} might have precluded the detailed analysis of I_{Kr} in this cell type. I_{Kr} current density (0.45 ± 0.03 pA pF⁻¹) in guinea-pig SA node cells is also much lower than that in atrial (2.53 pA pF⁻¹; Sanguinetti & Jurkiewicz, 1991) and ventricular cells (1.02 pA pF⁻¹; Sanguinetti & Jurkiewicz, 1990a) in the same species, while the I_{Ks} current density (8.71 ± 0.40 pA pF⁻¹) in SA node cells is comparable to that in ventricular cells (11.0 pA pF⁻¹; Sanguinetti & Jurkiewicz, 1990a) but lower than that in atrial cells (21.1 pA pF⁻¹, Sanguinetti & Jurkiewicz, 1991), thus showing that the I_{Kr} and I_{Ks} densities vary regionally within the same heart. In addition, the relative density of I_{Kr} to I_{Ks} in SA node cells (0.052) is lower than that in atrial (0.119; Sanguinetti & Jurkiewicz, 1991) and ventricular cells (0.093; Sanguinetti & Jurkiewicz, 1990a) in the guinea-pig heart.

Exposure to a specific I_{Kr} blocker E-4031 was found to initially delay the repolarization phase at potentials negative to approximately -30 mV without producing any appreciable effect on repolarization at more depolarized potentials in spontaneous action potentials (Fig. 7). These results strongly indicate that the late phase of repolarization (at potentials negative to -30 mV) leading to the maximal diastolic potential at around -60 mV is primarily produced by I_{Kr} and that the contribution of I_{Ks} to the late repolarization is either absent or, if any, very small in the spontaneous action potentials in guinea-pig SA node cells. In addition, the observation that the block of I_{Kr} preferentially affects the repolarization at these negative potentials appears to be consistent with the prominent inward rectifying property of I_{Kr} which minimizes the contribution of repolarizing outward current through I_{Kr} at depolarized potentials. The inward rectification of I_{Kr} in guinea-pig SA node cells can be accounted for by the voltage-dependent inactivation process (Fig. 4), as has been demonstrated in other cardiac cells (Shibasaki, 1987; Sanguinetti & Jurkiewicz, 1990a; Ono & Ito, 1995; Smith *et al.* 1996; Spector *et al.* 1996). The decrease in the action potential amplitude and overshoot in the presence of E-4031 (Fig. 7B, middle panel), which eventually leads to the arrest of spontaneous activity, is likely to be secondarily induced by the voltage-dependent inactivation of I_{CaL} associated with the depolarization of the maximum diastolic potential. In this preparation, it has been demonstrated that the transient outward current (I_{to}) is not detected (Guo *et al.* 1997). While the present study did not fully elucidate the role of I_{Ks} in the spontaneous action potentials, it is reasonable to speculate that I_{Ks} is, at least in part, responsible for the early phase of repolarization in guinea-pig SA node cells. It is of great interest to clarify the relative contribution of I_{Kr} and I_{Ks} to the early and late phases of repolarization of spontaneous action potentials in mammalian pacemaker cells.

Both I_{Kr} and I_{Ks} have been demonstrated to represent a potentially relevant target for the actions of neurotransmitters and drugs. In addition to the methanesulfonanilides, a relatively broad spectrum of medications, including some antiarrhythmic (Follmer & Colatsky, 1990), antihistamic (Rampe *et al.* 1993; Woosley, 1996), antibiotic (Daleau *et al.* 1995) and psychoactive agents (Drolet *et al.* 1999), have been demonstrated to preferentially block I_{Kr} and thereby to delay the cardiac

repolarization. In contrast, the stimulation of both β - and α -adrenoceptors was shown to selectively enhance I_{Ks} in cardiac cells (Sanguinetti *et al.* 1991; Tohse *et al.* 1992; Wang *et al.* 1994; Mamas *et al.* 1996), thus showing that I_{Ks} primarily represents a target for actions of sympathetic neurotransmitters. The prolongation of the refractory period induced by class III antiarrhythmic agents through the inhibition of I_{Kr} was demonstrated to be reversed by the enhancement of I_{Ks} by β -adrenergic stimulation (Sanguinetti *et al.* 1991), thus showing that the electrical activity of cardiac cells can be modulated by a differential regulation of two I_K components by neurotransmitters and drugs. Since both I_{Kr} and I_{Ks} are present and also appear to play a role in the development of pacemaker activity in guinea-pig SA node cells, these cell preparations may provide a suitable experimental model for future studies investigating the interactions of neurotransmitters and drugs affecting the I_K components in the SA node pacemaking activity.

REFERENCES

- ABBOTT, G.W., SESTI, F., SPLAWSKI, I., BUCK, M.E., LEHMANN, M.H., TIMOTHY, K.W., KEATING, M.T. & GOLDSTEIN, S.A.N. (1999). MiRP1 forms I_{Kr} potassium channels with HERG and is associated with cardiac arrhythmias. *Cell* **97**, 175-187.
- ANUMONWO, J.M.B., FREEMAN, L.C., KWOK, W.M. & KASS, R.S. (1992). Delayed rectification in single cells isolated from guinea pig sinoatrial node. *American Journal of Physiology* **262**, H921-925.
- BARHANIN, J., LESAGE, F., GUILLEMARE, E., FINK, M., LAZDUNSKI, M. & ROMÉY, G. (1996). K_v LQT1 and IsK (minK) proteins associate to form the I_{Ks} cardiac potassium current. *Nature* **384**, 78-80.
- BLEEKER, W.K., MACKAAY, A.J.C., MASSON-PEVET, M., BOUMAN, L.N. & BECKER, A.E. (1980). Functional and morphological organization of the rabbit sinus node. *Circulation Research* **46**, 11-22.
- CARMELIET, E. (1992). Voltage- and time-dependent block of the delayed K^+ current in cardiac myocytes by dofetilide. *Journal of Pharmacology and Experimental Therapeutics* **262**, 809-817.
- CURRAN, M.E., SPLAWSKI, I., TIMOTHY, K.W., VINCENT, G.M., GREEN, E.D. & KEATING, M.T. (1995). A molecular basis for cardiac arrhythmia: *HERG* mutations cause long QT syndrome. *Cell* **80**, 795-803.

- DALEAU, P., LESSARD, E., GROLEAU, M.-F. & TURGEON, J. (1995). Erythromycin blocks the rapid component of the delayed rectifier potassium current and lengthens repolarization of guinea pig ventricular myocytes. *Circulation Research* **91**, 3010-3016.
- DI FRANCESCO, D., FERRONI, A., MAZZANTI, M. & TROMBA, C. (1986). Properties of the hyperpolarizing-activated current (i_p) in cells isolated from the rabbit sino-atrial node. *Journal of Physiology* **377**, 61-88.
- DOERR, T., DINGER, R. & TRAUTWEIN, W. (1989). Calcium currents in single SA nodal cells of the rabbit heart studied with action potential clamp. *Pflügers Archiv* **413**, 599-603.
- DROLET, B., VINCENT, F., RAIL, J., CHAHINE, M., DESCHENES, D., NADEAU, S., KHALIFA, M., HAMELIN, B.A., & TURGEON, J. (1999). Thioridazine lengthens repolarization of cardiac ventricular myocytes by blocking the delayed rectifier potassium current. *Journal of Pharmacology and Experimental Therapeutics* **288**, 1261-1268.
- FREEMAN, L.C. & KASS, R.S. (1993). Delayed rectifier potassium channels in ventricle and sinoatrial node of the guinea pig: molecular and regulatory properties. *Cardiovascular Drugs and Therapy* **7**, 627-635.
- FOLLMER, C.H. & COLATSKY, T.J. (1990). Block of delayed rectifier potassium current, I_K , by flecainide and E-4031 in cat ventricular myocytes. *Circulation* **82**, 289-293.
- GINTANT, G.A. (1996). Two components of delayed rectifier current in canine atrium and ventricle: Does I_{Ks} play a role in the reverse rate dependence of class III agents? *Circulation Research* **78**, 26-37.

- GUO, J., MITSUIYE, T. & NOMA, A. (1997). The sustained inward current in sino-atrial node cells of guinea-pig heart. *Pflügers Archiv* **433**, 390-396.
- GUO, J., ONO, K. & NOMA, A. (1995). A sustained inward current activated at the diastolic potential range in rabbit sino-atrial node cells. *Journal of Physiology* **483**, 1-13.
- HAGIWARA, N., IRISAWA, H. & KAMEYAMA, M. (1988). Contribution of two types of calcium currents to the pacemaker potentials of rabbit sino-atrial node cells. *Journal of Physiology* **395**, 233-253.
- HAGIWARA, N., IRISAWA, H., KASANUKI, H. & HOSODA, S. (1992). Background current in sino-atrial node cells of the rabbit heart. *Journal of Physiology* **448**, 53-72.
- HAMILL, O.P., MARTY, A., NEHER, E., SAKMANN, B. & SIGWORTH, F.J. (1981). Improved patch-clamp techniques for high-resolution current recording from cells and cell-free membrane patches. *Pflügers Archiv* **391**, 85-100.
- HO, W.-K., EARM, Y.E., LEE, S.H., BROWN, H.F. & NOBLE, D. (1996). Voltage- and time-dependent block of delayed rectifier K⁺ current in rabbit sino-atrial node cells by external Ca²⁺ and Mg²⁺. *Journal of Physiology* **494**, 727-742.
- IRISAWA, H., BROWN, H.F. & GILES, W. (1993). Cardiac pacemaking in the sinoatrial node. *Physiological Reviews* **73**, 197-227.
- ISENBERG, G. & KLÖCKNER, U. (1982). Calcium tolerant ventricular myocytes prepared by preincubation in a 'KB medium'. *Pflügers Archiv* **395**, 6-18.

- ITO, H. & ONO, K. (1995). A rapidly activating delayed rectifier K^+ channel in rabbit sinoatrial node cells. *American Journal of Physiology* **269**, H443-452.
- ITO, H., ONO, K. & NOMA, A. (1994). Background conductance attributable to spontaneous opening of muscarinic K^+ channels in rabbit sino-atrial node cells. *Journal of Physiology* **476**, 55-68.
- LEI, M. & BROWN, H.F. (1996). Two components of the delayed rectifier potassium current, I_{K_r} , in rabbit sino-atrial node cells. *Experimental Physiology* **81**, 725-741.
- LI, G.-R., FENG, J., YUE, L., CARRIER, M. & NATTEL, S. (1996). Evidence for two components of delayed rectifier K^+ current in human ventricular myocytes. *Circulation Research* **78**, 689-696.
- LIU, D.-W. & ANTZELEVITCH, C. (1995). Characteristics of the delayed rectifier current (I_{K_r} and I_{K_s}) in canine ventricular epicardial, midmyocardial, and endocardial myocytes: A weaker I_{K_s} contributes to the longer action potential of the M cell. *Circulation Research* **76**, 351-365.
- MAMAS, M.A., CONNORS, S.C. & TERRAR, D.A. (1996). Effects of protein kinase C on the components of the delayed rectifier potassium current in guinea-pig isolated ventricular myocytes (abstract). *Journal of Physiology* **493.P**, 26P-27P.
- MATSUURA, H., EHARA, T. & IMOTO, Y. (1987). An analysis of the delayed outward current in single ventricular cells of the guinea-pig. *Pflügers Archiv* **410**, 596-603.
- NOBLE, D. & TSIEN, R.W. (1969). Outward membrane currents activated in the plateau range of potentials in cardiac Purkinje fibres. *Journal of Physiology* **200**, 205-231.

- ONO, K. & ITO, H. (1995). Role of rapidly activating delayed rectifier K^+ current in sinoatrial node pacemaker activity. *American Journal of Physiology* **269**, H453-462.
- OPTHÖF, T., DE JONGE, B., MACKAAY, A.J.C., BLEEKER, W.K., MASSON-PEVET, M., JONGSMA, H.J. & BOUMAN, L.N. (1985). Functional and morphological organization of the guinea-pig sinoatrial node compared with the rabbit sinoatrial node. *Journal of Molecular and Cellular Cardiology* **17**, 549-564.
- RAMPE, D., WIBLE, B., BROWN, A.M. & DAGE, R.C. (1993). Effects of terfenadine and its metabolites on a delayed rectifier K^+ channel cloned from human heart. *Molecular Pharmacology* **44**, 1240-1245.
- SANGUINETTI, M.C., CURRAN, M.E., ZOU, A., SHEN, J., SPECTOR, P.S., ATKINSON, D.L. & KEATING, M.T. (1996). Coassembly of K_v LQT1 and minK (IsK) proteins to form cardiac I_{Ks} potassium channel. *Nature* **384**, 80-83.
- SANGUINETTI, M.C., JIANG, C., CURRAN, M.E. & KEATING, M.T. (1995). A mechanistic link between an inherited and an acquired cardiac arrhythmia: *HERG* encodes the I_{Kr} potassium channel. *Cell* **81**, 299-307.
- SANGUINETTI, M.C. & JURKIEWICZ, N.K. (1990a). Two components of cardiac delayed rectifier K^+ current: Differential sensitivity to block by class III antiarrhythmic agents. *Journal of General Physiology* **96**, 195-215.
- SANGUINETTI, M.C. & JURKIEWICZ, N.K. (1990b). Lanthanum blocks a specific component of I_K and screens membrane surface charge in cardiac cells. *American Journal of Physiology* **259**, H1881-H1889.

- SANGUINETTI, M.C. & JURKIEWICZ, N.K. (1991). Delayed rectifier outward K^+ current is composed of two currents in guinea pig atrial cells. *American Journal of Physiology* **260**, H393-H399.
- SANGUINETTI, M.C., JURKIEWICZ, N.K., SCOTT, A. & SIEGL, P.K.S. (1991). Isoproterenol antagonizes prolongation of refractory period by the class III antiarrhythmic agent E-4031 in guinea pig myocytes. Mechanism of action. *Circulation Research* **68**, 77-84.
- SHIBASAKI, T. (1987). Conductance and kinetics of delayed rectifier potassium channels in nodal cells of the rabbit heart. *Journal of Physiology* **387**, 227-250.
- SMITH, P.L., BAUKROWITZ, T. & YELLEN, G. (1996). The inward rectification mechanism of the HERG cardiac potassium channel. *Nature* **379**, 833-836.
- SPECTOR, P.S., CURRAN, M.E., ZOU, A., KEATING, M.T. & SANGUINETTI, M.C. (1996). Fast inactivation causes rectification of the I_{Kr} channel. *Journal of General Physiology* **107**, 611-619.
- TOHSE, N., NAKAYA, H. & KANNO, M. (1992). α_1 -adrenoceptor stimulation enhances the delayed rectifier K^+ current of guinea pig ventricular cells through the activation of protein kinase C. *Circulation Research* **71**, 1441-1446.
- TRUDEAU, M.C., WARMKE, J.W., GANETZKY, B. & ROBERTSON, G.A. (1995). HERG, a human inward rectifier in the voltage-gated potassium channel family. *Science* **269**, 92-95.
- VERHEIJCK, E.E., VAN GINNEKEN, A.C.G., BOURIER, J. & BOUMAN, L.N. (1995). Effects of delayed rectifier current blockade by E-4031 on impulse generation in single sinoatrial nodal myocytes of the rabbit. *Circulation Research* **76**, 607-615.

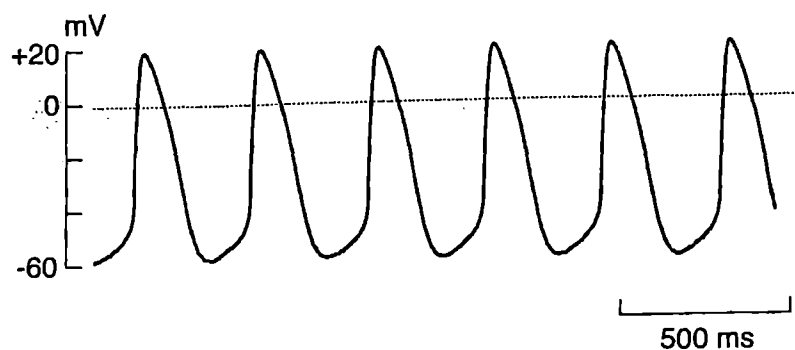
WANG, Z., FERMINI, B. & NATTEL, S. (1994). Rapid and slow components of delayed rectifier current in human atrial myocytes. *Cardiovascular Research* **28**, 1540-1546.

WOOSLEY, R.L. (1996). Cardiac actions of antihistamines. *Annual Review of Pharmacology and Toxicology* **36**, 233-252.

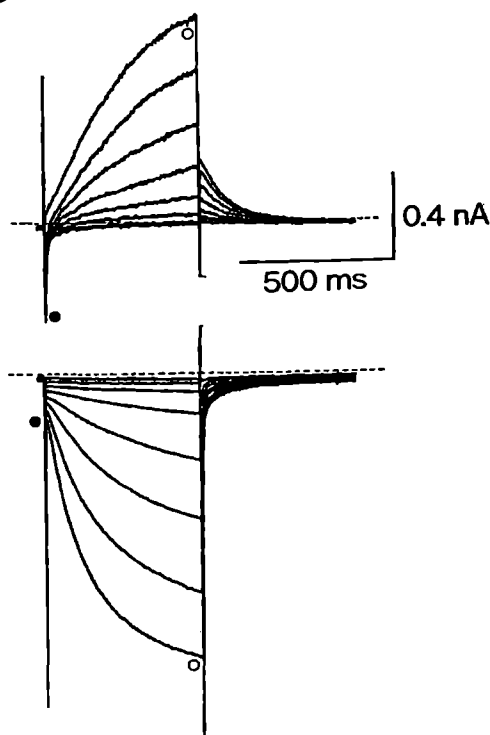
ZHOU, Z. & LIPSUS, S.L. (1994). Delayed rectifier potassium current (I_K) in latent atrial pacemaker cells isolated from cat right atrium. *Pflügers Archiv* **426**, 341-347.

Acknowledgements

This study was supported by Grants-in-Aid for Scientific Research (C) (Nos. 08670057, 09670048 and 11670040 to H.M.) from the Ministry of Education, Science, Sports and Culture of Japan. The authors thank Prof. A. Noma (Kyoto University, Japan) for teaching the method for isolating guinea-pig sino-atrial node cells, Dr. T. Shioya (Saga Medical School, Japan) for providing us with the computer programs used for the data analysis, Dr. B. Quinn for critically reading the manuscript and Ms. Y. Tanigaki for secretarial assistance.



B



C

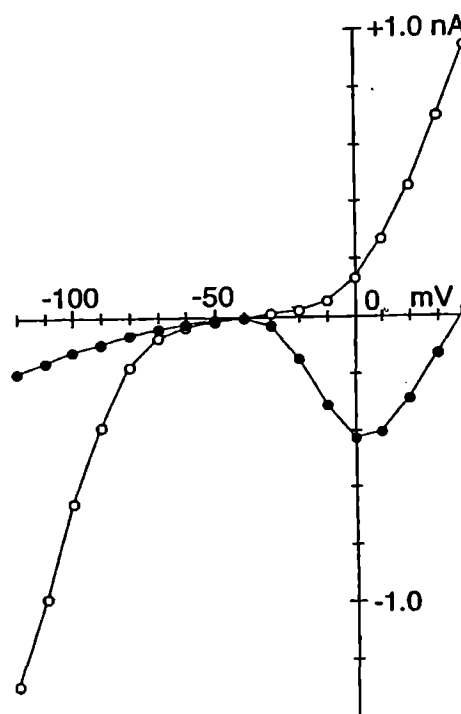


Figure 1. Membrane potential and whole-cell currents recorded from an isolated guinea-pig SA node pacemaker cell

A, spontaneous action potentials recorded from a regularly contracting SA node cell in the normal Tyrode solution under the current-clamp mode. Maximum diastolic potential, -58 mV; beat rate, 178 min^{-1} . B, superimposed current traces elicited by 500-ms command steps to membrane potentials of -30 to $+40$ mV (top) and -50 to -120 mV (bottom) in 10 mV steps applied from a holding potential of -40 mV. The dotted lines indicate the zero-current level. These voltage-clamp records were obtained from the same cell as in A. C, current-voltage (I - V) relationships measured at the initial (\bullet) and end (\circ) of 500-ms voltage steps. Initial current was measured either at peak of the I_{CaL} during the depolarizing test pulse or immediately after a decay of the capacitance transient during the hyperpolarizing test pulse. The late current was measured near the end of 500-ms voltage step. Continuous lines through data points were fitted by eye.

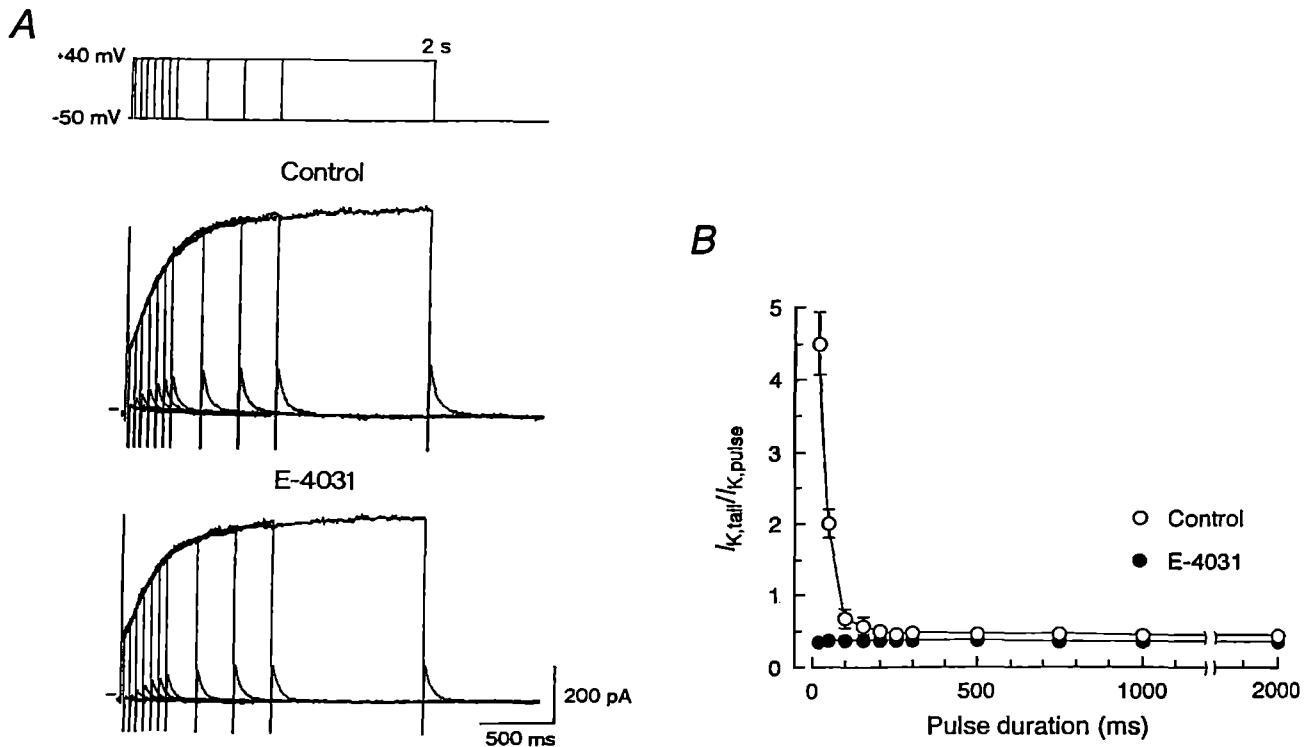


Figure 2. Envelope of tails test for I_K under control conditions and during exposure to E-4031

A, voltage protocol (top) and superimposed current traces elicited by depolarizing pulses from a holding potential of -50 mV to +40 mV for various durations (20, 60, 100, 150, 200, 250, 300, 500, 750, 1000 and 2000 ms) under control conditions (middle) and after 3 min exposure to 5 μ M E-4031 (bottom). The zero-current level is indicated to the left of the current records by the horizontal line. B, ratio of peak tail current amplitude elicited upon return to a holding potential of -50 mV ($I_{K,tail}$) to the amplitude of time-dependent currents activated during the depolarizing test pulses ($I_{K,pulse}$) plotted as a function of pulse duration, under control conditions (○) and during the exposure to E-4031 (●). $I_{K,tail}$ was determined by digitally subtracting the steady-state current level from the peak current level measured after the step to a holding potential of -50 mV. $I_{K,pulse}$ was determined by digital subtraction of the current level measured after a decay of the capacitance transient from that at the end of the depolarizing pulse. Data represent the means \pm S.E.M. of three cells.

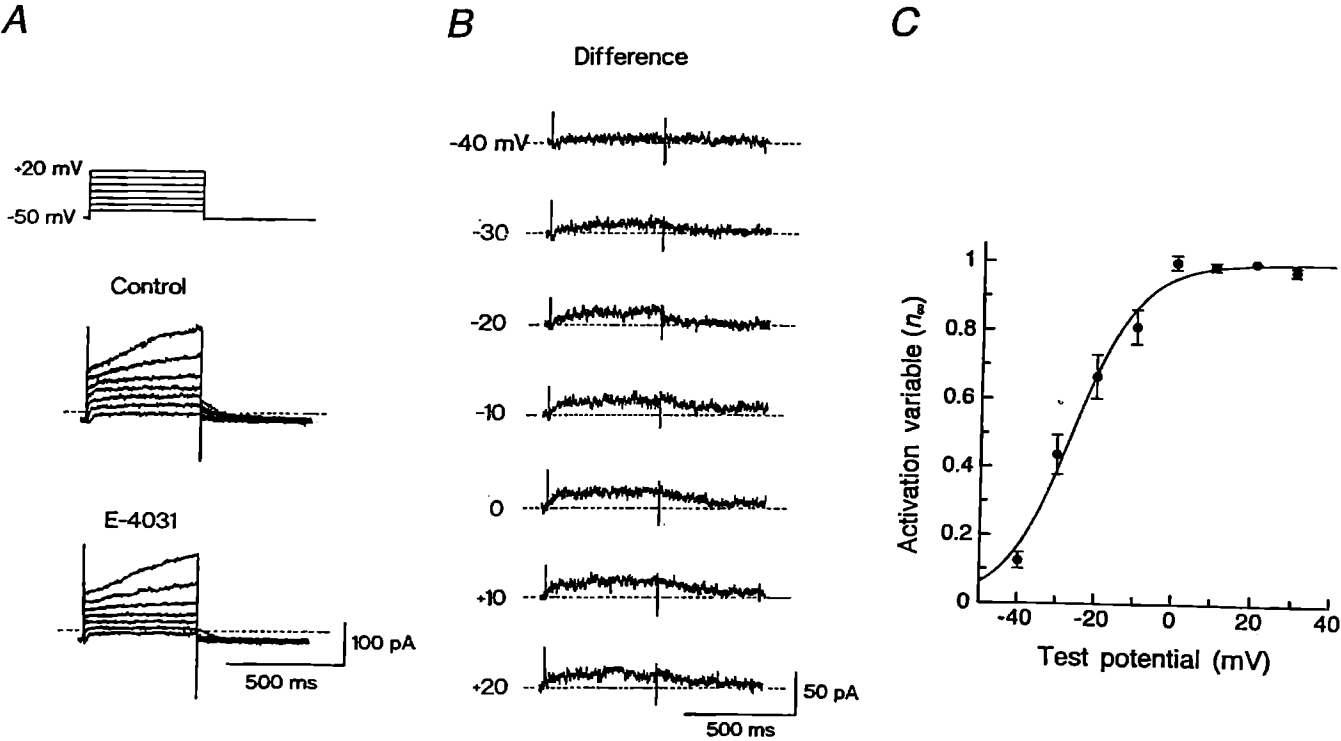


Figure 3. Voltage-dependence of I_{Kr} activation

A, voltage-clamp protocol (top) and superimposed current traces in response to 500 ms voltage steps to membrane potentials of -40 to $+20$ mV applied in 10 mV steps from a holding potential of -50 mV, under control conditions (middle) and during the exposure to $5 \mu\text{M}$ E-4031 (bottom). B, I_{Kr} obtained by digitally subtracting the current trace in the presence of E-4031 from the control trace at each test potential, shown in A. C, peak amplitude of I_{Kr} tail currents elicited upon return to the holding potential was normalized with reference to its amplitude at $+20$ mV and was plotted against the test potential. The continuous curve was drawn by a least-squares fit of a Boltzmann equation yielding $V_{1/2}$ of -26.2 mV and k of 8.7 mV (see text). Data represent the means \pm S.E.M. of three cells.

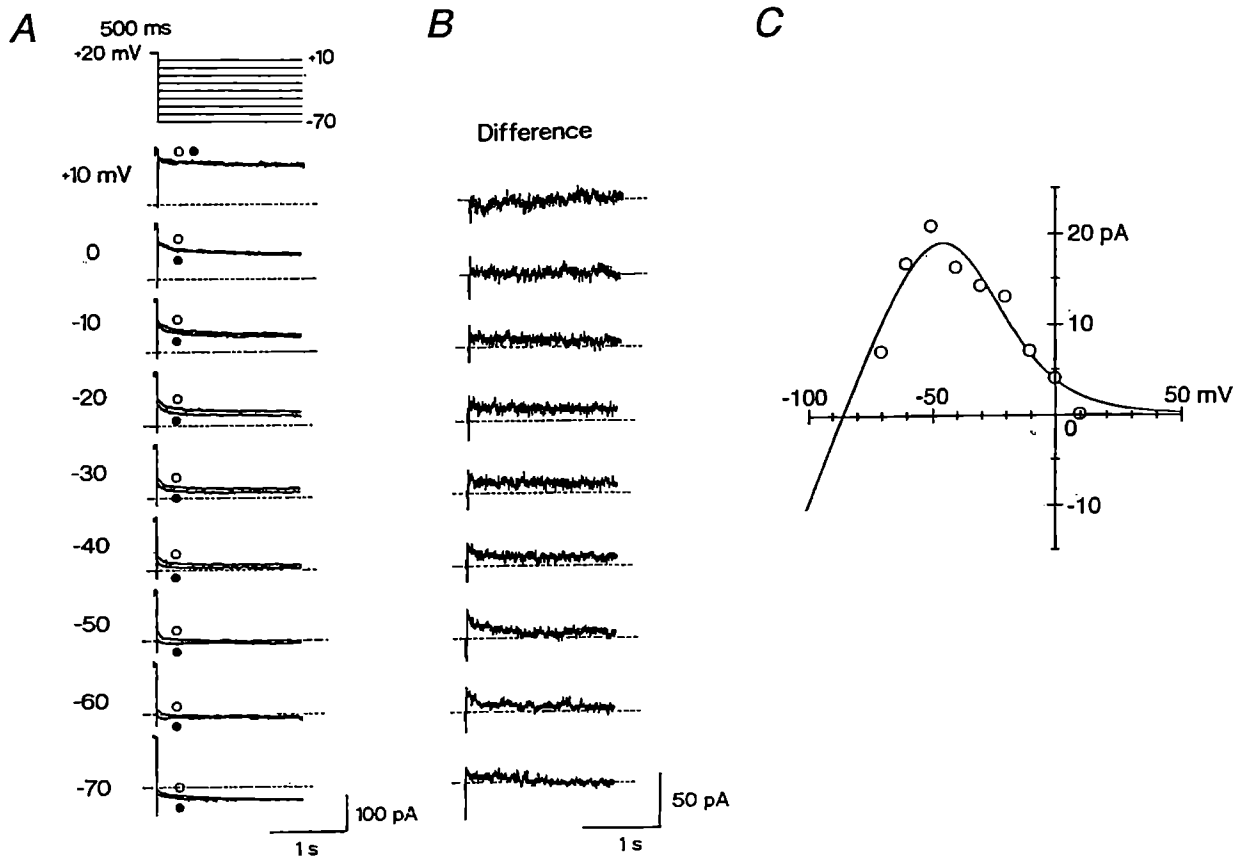


Figure 4. Inwardly rectifying properties of I_{Kr} .

A, voltage-clamp protocol (top) and the membrane currents elicited by 2-s voltage-steps to potentials of +10 to -70 mV in 10 mV steps after 500-ms depolarization to +20 mV. Membrane currents were recorded at all test potentials initially in the absence of 5 μ M E-4031 (O) and then during its presence (●). Test potential is indicated to the left of the current traces. Dotted line indicates the zero-current level (also in B). B, difference current at each test potential obtained by digital subtraction of current trace in the presence of E-4031 (●) from that in its absence (O), shown in A. C, peak amplitudes of I_{Kr} tail currents plotted as a function of the test potentials. A solid line through the data points shows the least-squares fit of Eqs (2) and (3).

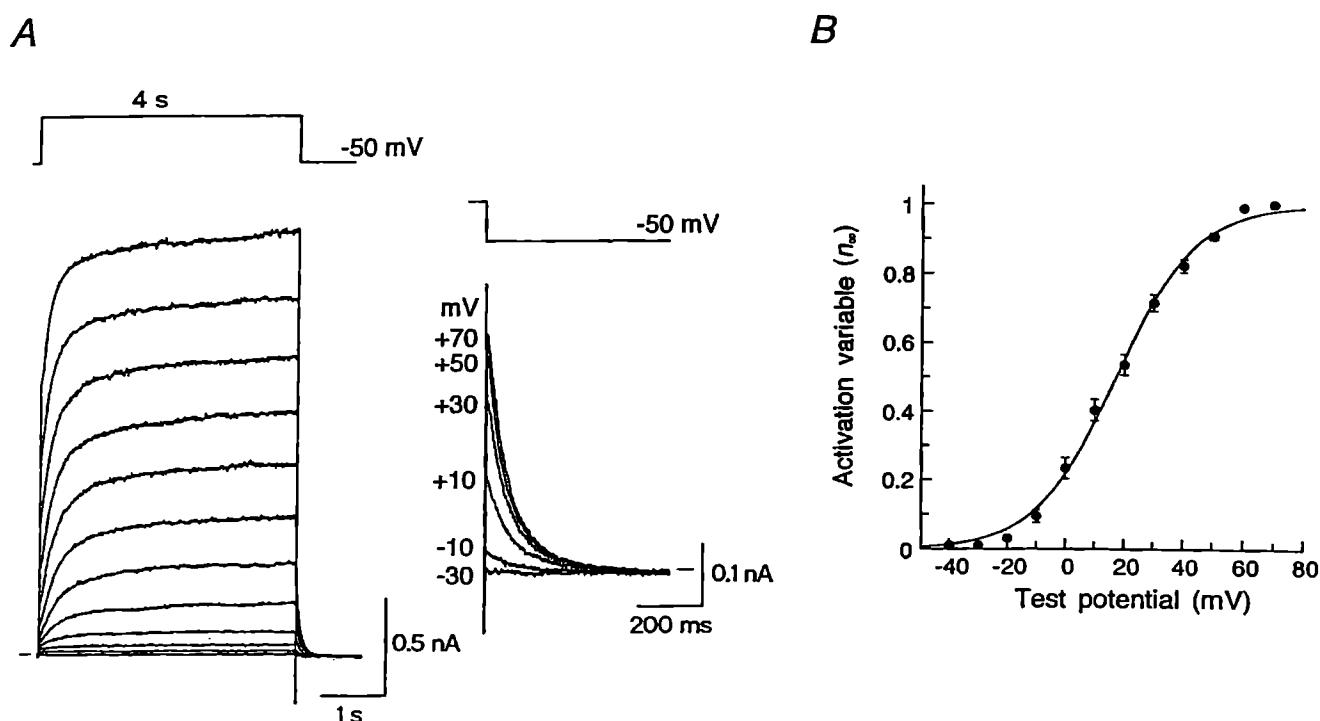


Figure 5. Voltage dependence of I_{K_s} activation

A, current traces during 4-s voltage-clamp steps to membrane potentials of -40 to $+70$ mV in 10 mV steps applied from a holding potential of -50 mV. These recordings were conducted in the presence of $5 \mu\text{M}$ E-4031 to inhibit I_{K_r} . Tail currents elicited after depolarizing steps to -30 , -10 , $+10$, $+30$, $+50$ and $+70$ mV were illustrated on an expanded scale (inset). Zero-current level is indicated to either the left or the right (inset) of current traces by a horizontal bar. B, amplitude of I_{K_s} tail current at each test potential was normalized to the maximum amplitude at $+70$ mV and then was plotted as a function of test potential. Data points were fitted to the Boltzmann equation (Eq 1) using the least-squares method with $V_{1/2}$ of $+17.2$ mV and k of 13.5 mV (see text). Data represent the means \pm S.E.M. of three cells.

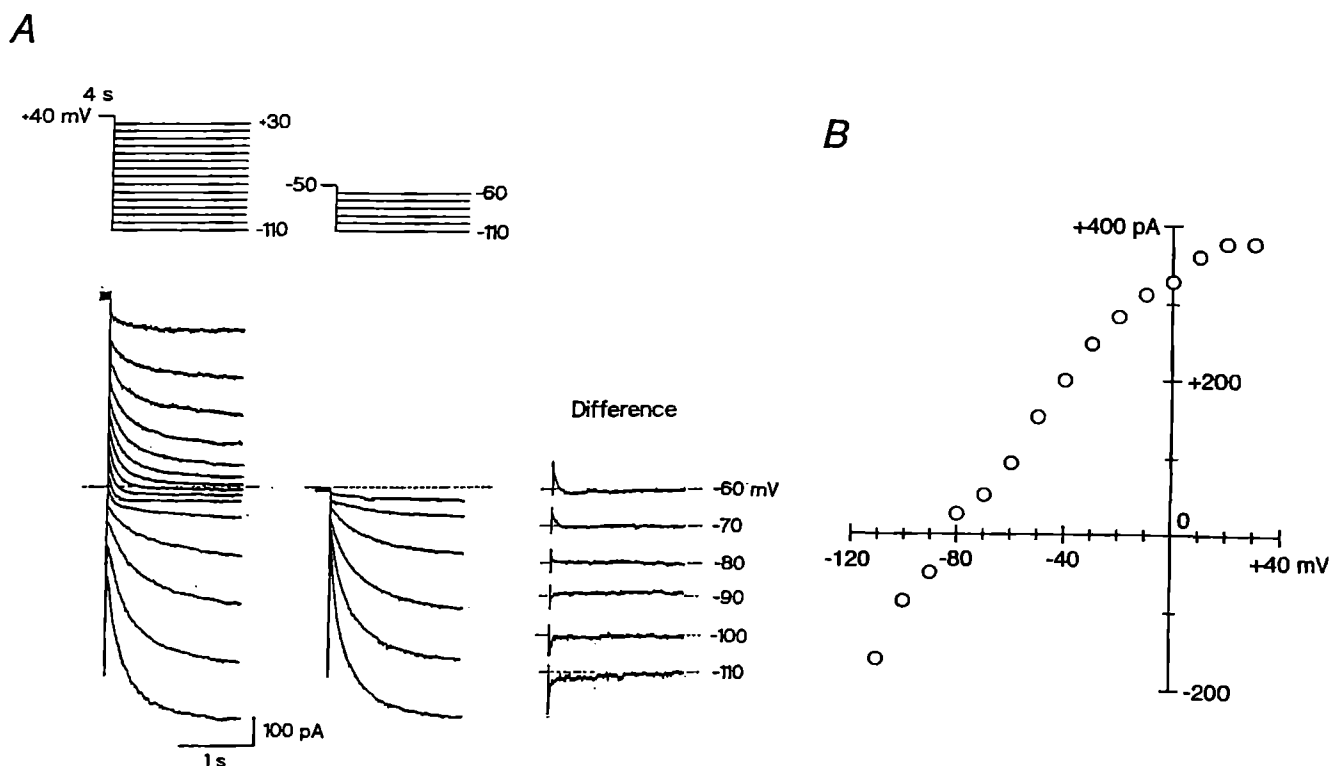


Figure 6. Conduction properties of I_{Ks} in guinea-pig SA node cells

A, cell was depolarized from a holding potential of -50 mV to +40 mV for 4 s to activate I_{Ks} and then was repolarized to various test potentials between +30 and -110 mV in 10 mV steps (left panel). The same cell was repolarized from the -50 mV holding potential to membrane potentials between -60 and -110 mV without the depolarizing pulse (middle). I_{Ks} tail current elicited on return to the test potentials between -60 and -110 mV after a 4-s depolarizing pulse to +40 mV was determined by subtracting membrane current without the depolarizing pulse to +40 mV from that with the depolarizing pulse (right). A schematic diagram of the voltage protocol is given above the current traces. These recordings were conducted in the presence of 5 μ M E-4031 to inhibit I_{Kr} . The dotted line indicates the zero-current level. B, amplitude of I_{Ks} tail current at each test potential was divided by the expected decrease in the activation variable and then was plotted as a function of the membrane potential.

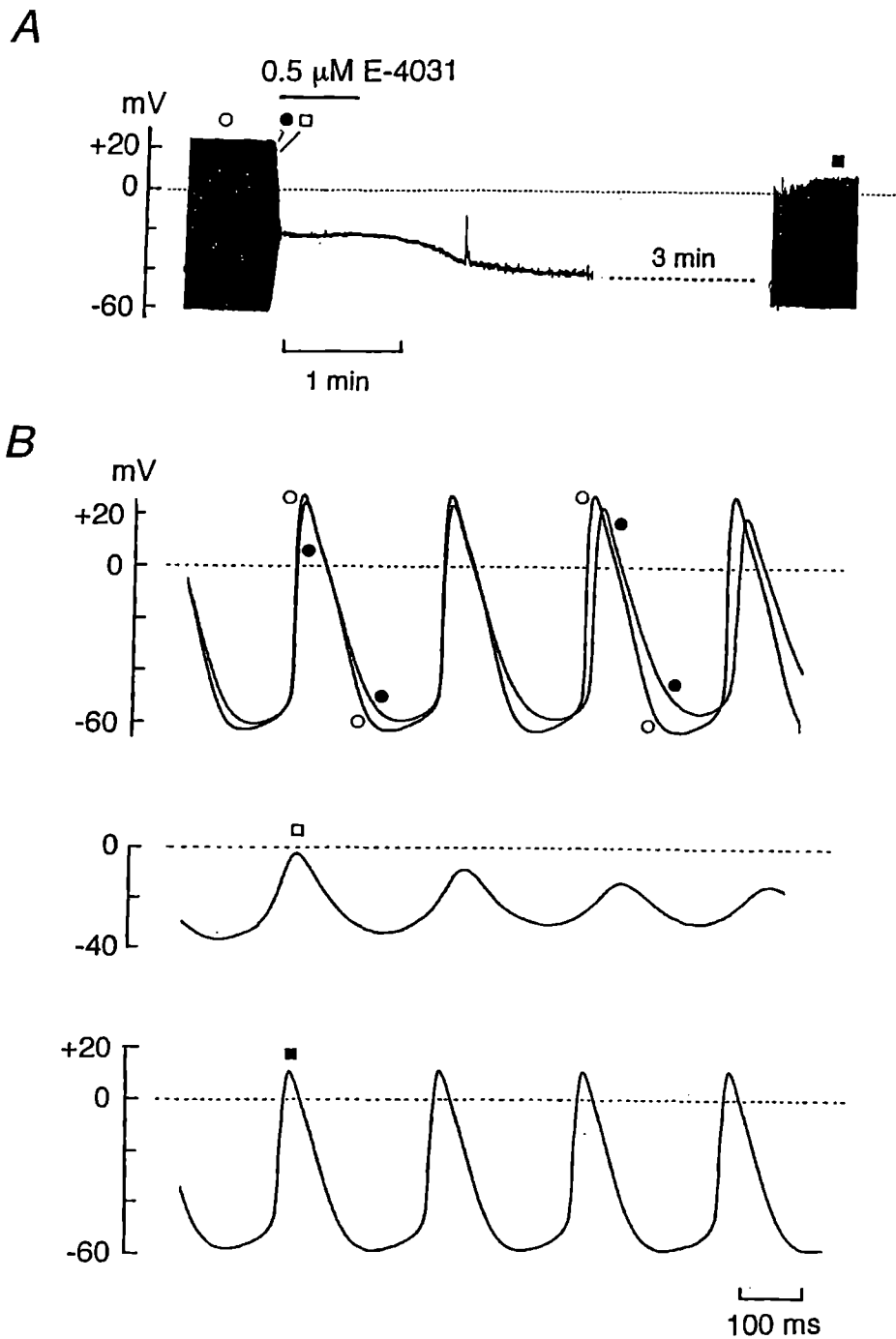


Figure 7. Effect of block of I_{K_r} by E-4031 on the spontaneous activity

A, chart record of membrane potential before, during the exposure to and after washing off 0.5 μ M E-4031. E-4031 was added to normal Tyrode solution during the period indicated by the horizontal bar. B, action potentials on a faster time scale recorded before (upper panel, O), 3 s (upper, ●) and 6 s (middle, □) after exposure to E-4031, and about 6 min after washing the drug off (lower, ■).

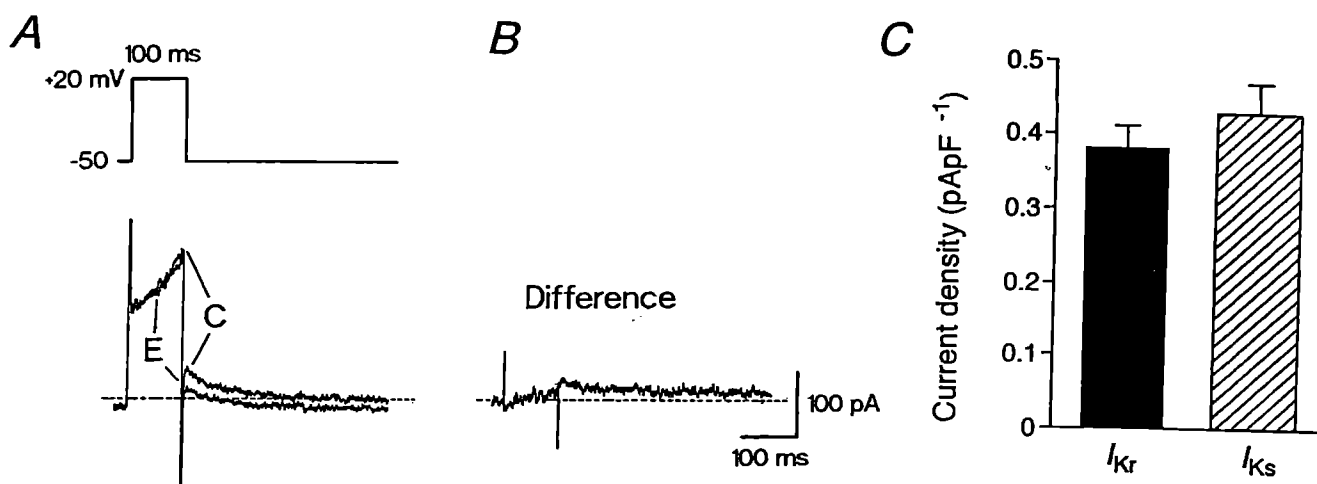


Figure 8. Comparison of amplitude of I_{Kr} and I_{Ks} during the voltage-clamp protocol simulating the action potential

A, voltage-clamp protocol (top) and corresponding currents (bottom) before (C) and during exposure to 5 μ M E-4031 (E). Note that the E-4031-resistant current, which is present during exposure to E-4031 (denoted as E), corresponds to I_{Ks} . B, I_{Kr} obtained by digital subtraction of the current during exposure to E-4031 from that before exposure, shown in A. C, amplitudes of tail currents of I_{Kr} and I_{Ks} (n = 4 cells), elicited on repolarization to -50 mV after 100-ms step to +20 mV. The columns and bars represent the means and S.E.M., respectively, and there was no significant difference between the two groups (Student's paired *t* test).